Multi-axis Force Sensing with Pre-stressed Resonant Composite Plates : An Alternative to Strain Gauge Force Sensors/

Davinson Castano Cano, Mathieu Grossard, Arnaud Hubert

Multi-axis Force Sensing with Pre-stressed Resonant Composite Plates: An Alternative to Strain Gauge Force Sensors

Davinson CASTAÑO-CANO[1,2], Mathieu GROSSARD[1] and Arnaud HUBERT[2]

Abstract— **Industrial robots embedding multi-axis force sensors at the robot/environment interface presents numerous advantages in terms of safety, dexterity and collaborative perspectives. The key-point of these developments remains the availability of cheap but sufficiently precise multi-axis force sensors. This paper proposes a model-based approach to design a new alternative to commonly used strain gauge sensors. The principle of the device relies on pre-stress resonant composite plates where feedback control and measurement are achieved with piezoelectric transducers. The main originality of this work is that the force to be measured may present multi-axis components. Based on pre-stress and piezoelectric theories, a complete electromechanical model is proposed. This one is used during the design of a resonating composite *Mindlin* plate, embedding piezoelectric patches. It is shown that the effects of in-plane and out-of-plane external forces can be considered as pre-stress components. These ones, at the root of buckling phenomena, alter the stiffness of the structure and shift the plate resonance frequencies. Then, by solving the eigenvalue problem of the pre-stress vibrating structure, we can find the relationship between the natural frequencies of the structure and the externally applied multi-axis force. The proof of concept of this sensor is achieved on a case study. Finally, numerical results from both, *home-made* and commercial, finite element software demonstrates the interest of our approach to design integrated and inexpensive multi-axis force sensors solutions.**

I. INTRODUCTION

Future challenges for industrial robotics concern mainly interactive, collaborative and safe robotics. In these perspectives, the ability to sense the arm-environment interactions is a crucial need. This is even the key-point for robots to evolve from purely repetitive behaviours to some degree of autonomy in unstructured surroundings and safe collaboration with humans [1], [2]. These needs for accurate force/torque sensors have become the object of numerous research approaches in the literature [3].

Principles and technologies exploited for the sensor, as well as its functional integration into the sensor body device, remain key factors to define the performance and modality of the design (e.g. optical-based force sensors [4], sensing capacitance array [5], modularized assembly of 1-D force sensors [6], structures based on parallel *Stewart* kinematics [7], etc.). Currently, the majority of available force sensors employ strain gauges mounted on more or less conventional mechanisms (e.g. shear-type rosette strain gauges fixed onto torsion bars [8] or Hollow Hexaform structures [9] for torque sensors, Maltese cross shape for force sensors [10], etc.), which can be fairly stiff and robust. However, strain-gauge-based sensors present drift problems and their manufacturing is process intensive (severe and precise requirements on the working, assembly and calibration of the integrated structure are needed). An attractive alternative to strain-gauge technology for force measurement are resonant-based sensors. Indeed, a great advantage lies in their easy way to measure frequency shift, and their reduced manufacturing cost. Moreover, resonant force sensors present advantages over static sensors in terms of noise immunity, high sensibility and good stability.

Because induced static stresses due to external forces slightly change the stiffness properties of the forced-vibrating structure, a slight frequency variation occurs. This results from the non-linearity of the strain field according to the external mechanical loads. Piezoelectric transducers, with their advantageous reversible (inverse and direct) electromechanical coupling effect, are usually employed in the force measurement principle based on integrated resonant sensors. Major studies currently found in literature about resonant-operating structures with multifunctional PZT patches rely on axially loaded beam elements [11], [12]. Nevertheless, this design limits the force sensing capabilities to only one direction for each beam. This choice for one-axis sensor design can be explained mostly by drastic complications encountered by the design of multi-axis piezoelectric resonators. To exhibit interesting modal sensitivities to forces along many preferential sensing directions, a more complex geometry must be envisaged than simple beams.

The idea proposed in this paper is to exploit different resonant modes of a single composite plate as a way to measure the components of an externally applied force. A review of the literature shows that no previous paper have investigated the vibrations of composite plates with piezoelectric transducers, taking into account the effects of in-plane and out-of-plane forces. Force sensing capabilities of plates, as a multi-axis extension of beam's force sensing capabilities, have not been yet exploited. The mechanical pre-stress theory proves that forces in all directions can be measured [13]. The simple shape of a plate is easily manufactured, all the more that piezoelectric actuators and sensors patches can simply be bonded to the upper and lower faces of the plate. This simple structure avoids the complex spatial arrangement of 1D resonating beams [14] or the difficulty to accurately sticking many strain gauges on different faces of squared cross-section beams [3]. The ef-

[1] Interactive Robotics Laboratory, LIST, CEA, Gif-sur-Yvette, F-91190, France. e-mails: davinson.castanocano@cea.fr mathieu.grossard@cea.fr

[2] Automatic Control and Micro-Mechatronic Systems Department, FEMTO-ST Institute, Université de Franche-Comté, ENSMM-UTBM-CNRS, Besançon, France. arnaud.hubert@femto-st.fr

fects of in-plane (membrane effect) and out-of-plane external forces generate a pre-stress of the structure. These ones, at the root of buckling phenomena, alter the global stiffness of the structure and shift the plate resonance frequencies. A complete electromechanical model is established in this paper to design pre-stress and resonating composite *Mindlin* plate embedding piezoelectric transducers. The model makes use of the *Hamilton*'s principle and energetic methods. Then, by solving the eigenvalue problem of the pre-stress vibrating structure, we can find the relationship between the natural frequencies of the structure and the externally applied multi-axis force. Due to the complexity of the computation, the eigenvalues of the resulting multiphysics problem is solved using an *home-made* finite element (FE) approximation.

The paper is organized as follows. In the next section, the model of the dynamic pre-stressed multilayer structure with piezoelectric transducers is established using variational principle. It explains how pre-stress phenomena influence the overall structure stiffness. In the third section, a FE formulation is proposed for *Mindlin* plate. Governing matrix equations of the full system are exposed. In the last section, a design approach for resonant force sensing is proposed through a case study. Our procedure to determine the applied multi-axis loads is finally validated by comparison with a commercial FE software.

II. Modelling of Active Structures with Pre-stress

Resonant force sensing is based on a mechanical structure whose natural frequencies and shapes are responsive to an external force (named $\mathring{F}$ in the paper). Such force is considered as parts of the boundary conditions of the structure. The main idea lies on the fact that frequencies and modal shapes of a structure are strongly dependant on their boundary conditions (force or displacement).

A. Description of the Structure

The sensor device is a composite structure made with a structural plate and a set of piezoelectric sensors and actuators. The simplified design of this system is displayed in Fig. 1. Different boundary conditions are imposed (*Dirichlet*/essential conditions on displacements or *Neumann*/natural conditions on forces). Boundary forces are measured using the resonance frequencies shift. It has to be noticed that two kinds of forces are considered:

- The excitation force $\tilde{F}^{ext}$ appears at high frequency. $\tilde{F}^{ext}$ will be created with piezoelectric elements to excite the resonances of the structure. The resonances can be obtained by application of electric potential to the piezoelectric patch electrodes.
- The to-be-measured force $\mathring{F}$ appears at a relatively low frequency. The relation between an applied to-be-measured force $\mathring{F}$ and the frequency shift of the structure can be understood via pre-stress loads. Indeed, in interactive robotics application and on the contrary of other forces $\tilde{F}^{ext}$, the frequencies of to-be-measured force $\mathring{F}$ are far below the resonant frequencies of the plate. In such a case, they can be considered as quasi-static forces that only affect the mean strain of the plate.

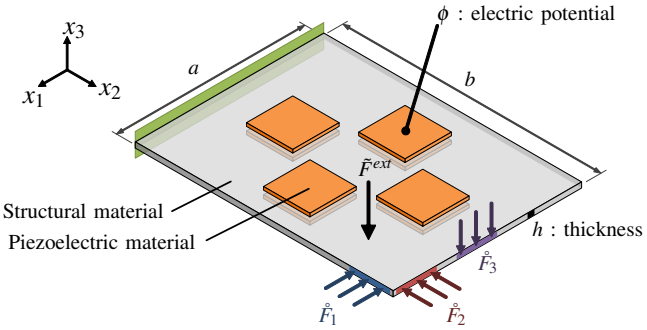

Fig. 1. Description of the force sensor composite structure (in-plane dimensions length a and width b, thickness h). The system is made from a structural plate with collocated piezoelectric transducers for actuation and sensing. A set of forces $\mathring{F} = \{\mathring{F}_1, \mathring{F}_2, \mathring{F}_3\}$ to be measured in different directions is applied at the edges of the plate (parts of boundary conditions).

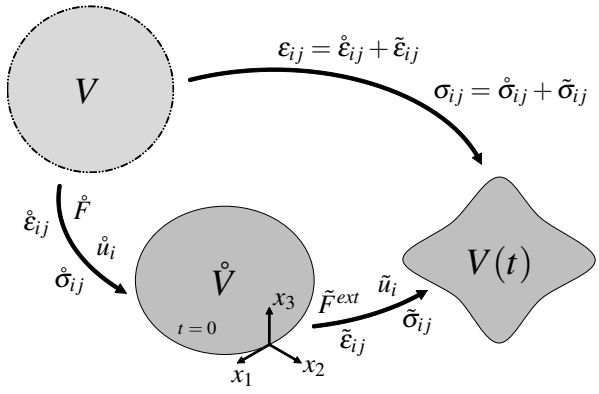

Fig. 2. The continuous volume V in a free state, is submitted to a pre-load $\mathring{F}$, that generates strain $\mathring{\varepsilon}$ and stress $\mathring{\sigma}$ into the body. The resulting configuration $\mathring{V}$ is therefore seen as the initial configuration ($t = 0$), from which, this body is excited to its resonance in response to external forces $\tilde{F}^{ext}$.

This frequency separation creates two groups of external forces, low-frequency forces that will shift the resonance and high-frequencies forces that will put the plate into resonance. The main characteristics of the plate can then be split into two terms, quantities only due to pre-stress (shown with $\mathring{}$), and quantities due to others sources (shown with $\tilde{}$) [15]. For example, the strain can be split as $\varepsilon_{ij} = \mathring{\varepsilon}_{ij} + \tilde{\varepsilon}_{ij}$ where $\mathring{\varepsilon}_{ij}$ is the pre-stress *quasi-static* contribution due to $\mathring{F}$ and $\tilde{\varepsilon}_{ij}$ a strain variation (due to $\tilde{F}^{ext}$) around the pre-stress configuration (Fig. 2).

According to the *Green-Lagrange* definition [16], the strain ε_{ij} in a continuous media is expressed in terms of its displacement u_i as :

$$\varepsilon_{ik} = \underbrace{\frac{1}{2}\left(\frac{\partial u_i}{\partial x_k} + \frac{\partial u_k}{\partial x_i}\right)}_{\varepsilon_{ik}^{(1)}} + \underbrace{\frac{1}{2}\frac{\partial u_l}{\partial x_i}\frac{\partial u_l}{\partial x_k}}_{\varepsilon_{ik}^{(2)}} \tag{1}$$

Einstein's summation convention on repeated indexes is used in this paper. Scientific literature [15] shows that in pre-stress structures, the main new contributions arise from

TABLE I
NOMENCLATURE

Symbol	Description
c	Elasticity modulus
D	Electrical displacement field
E	Electric field
e	Piezoelectric material matrix
F_V, F_S, F_P	Body, Surface, Punctual forces
K	Stiffness matrix
K_g	Geometric matrix
M	Mass matrix
Q	Electric charge
$\bar{q}$	Electric charge density
$\mathscr{U}$	Internal energy density
$V, \mathring{V}$	Body free of any load, and pre-stressed body
$\mathfrak{e}$	Permittivity
ε	Mechanical strain
σ	Mechanical stress
ρ	Mass density
ϕ	Electric potential
θ_x, θ_y	Angles
$\mathring{}$	Over-script for pre-stress terms
$\tilde{}$	Over-script for excitation terms

quadratic terms $\varepsilon_{ik}^{(2)}$ that are often neglected in linear non-pre-stress mechanical problems. Therefore, the two terms $\varepsilon_{ik}^{(1)}$ and $\varepsilon_{ik}^{(2)}$ will be kept in the following sections. A brief description of each symbol used in the paper is shown in Table I.

B. Internal Energy for Passive Pre-stress Structures

Elastic energy density $\mathscr{U}_m$ of continuous media results from an integration of stress σ along strain ε:

$$\mathscr{U}_m = \int_0^{\varepsilon_{ij}} \sigma_{ij}\, d\varepsilon_{ij} \tag{2}$$

If stress and strain are split according to Fig. 2 (e.g. $\sigma_{ij} = \mathring{\sigma}_{ij} + \tilde{\sigma}_{ij}$ and $\varepsilon_{ij} = \mathring{\varepsilon}_{ij} + \tilde{\varepsilon}_{ij}$) and linear elastic constitutive law is assumed (*Hooke*'s law: $\sigma_{ij} = c_{ijkl}\,\varepsilon_{kl}$), $\mathscr{U}_m$ becomes:

$$\mathscr{U}_m = \underbrace{\frac{1}{2}\, c_{ijkl}\, \mathring{\varepsilon}_{ij}\, \mathring{\varepsilon}_{kl}}_{\mathring{\mathscr{U}}_k} + c_{ijkl}\, \mathring{\varepsilon}_{ij}\, \tilde{\varepsilon}_{kl} + \frac{1}{2} c_{ijkl}\, \tilde{\varepsilon}_{ij}\, \tilde{\varepsilon}_{kl} \tag{3}$$

In this expression, $\mathring{\mathscr{U}}_k$ is a constant term. Other terms can be expanded considering entire definition of the *Green-Lagrange* strain (1) :

$$\begin{aligned} \mathscr{U}_m = & \underbrace{\frac{1}{2}\, c_{ijkl}\, \mathring{\varepsilon}_{ij}\, \mathring{\varepsilon}_{kl}}_{\mathring{\mathscr{U}}_k} + \underbrace{\frac{1}{2}\, c_{ijkl}\, \tilde{\varepsilon}_{ij}^{(1)}\, \tilde{\varepsilon}_{kl}^{(1)}}_{\mathscr{U}_k} + \underbrace{\mathring{\sigma}_{ij}\, \tilde{\varepsilon}_{ij}^{(1)}}_{\mathscr{U}_n} + \underbrace{\mathring{\sigma}_{ij}\, \tilde{\varepsilon}_{ij}^{(2)}}_{\mathscr{U}_g} \\ & + \underbrace{c_{ijkl}\, \tilde{\varepsilon}_{ij}^{(1)}\, \tilde{\varepsilon}_{kl}^{(2)} + \frac{1}{2}\, c_{ijkl}\, \tilde{\varepsilon}_{ij}^{(2)}\, \tilde{\varepsilon}_{kl}^{(2)}}_{\mathscr{U}_{nl}} \end{aligned} \tag{4}$$

The second term $\mathscr{U}_k$ is the classic first-order elastic strain energy density for non-pre-stress structure. As explained in [15] and due to an internal equilibrium (force balance), the third term $\mathscr{U}_n$ disappears when we consider the total energy of the system. The forth term, a second-order strain contribution, is known as the energy density of pre-stress [13] or the geometric energy density $\mathscr{U}_g$ [15] (geometric because it does not depend on the material of the structure). This term will be exploited in the principle of our force sensor because it is directly related to the to-be-measured force $\mathring{F}$ (through the term $\mathring{\sigma}$). Finally the last higher-order terms (3^{rd} and 4^{th} order) named $\mathscr{U}_{nl}$, are required in the case of large displacements (i.e. for out-of-plane motions when small strain and small displacements theory is no longer valid).

C. Internal Energy for Piezoelectric Structures

Such force sensor device is therefore a sandwich compound of different materials (a passive structural plate where piezoelectric transducers are integrated, Fig. 1). Piezoelectric transducers are needed to generate the excitation $\tilde{F}^{ext}$ that puts the structural system in resonance.

- Piezoelectric actuators are dynamically excited to produce shear forces at the upper face of the plate.
- Piezoelectric sensors permit to measure structural response in terms of surface strain.

Where piezoelectric materials are present, the previous internal energy density has to be completed with the electric terms [17]:

$$\mathscr{U} = \frac{1}{2}\left(\varepsilon_{ij}\sigma_{ij} - E_i D_i\right) \tag{5}$$

If linear piezoelectric constitutive equations are assumed (superscript ^{E} stands for constant electric field, and $^\varepsilon$ stands for constant strain) [18], [19]:

$$\begin{aligned} \sigma_{ij} &= c_{ijkl}^E\, \varepsilon_{kl} - e_{kij}\, E_k \\ D_i &= e_{ikl}\, \varepsilon_{kl} + \mathfrak{e}_{ij}^\varepsilon\, E_j \end{aligned} \tag{6}$$

the internal energy density of piezoelectric parts becomes:

$$\mathscr{U} = \underbrace{\frac{1}{2}\, c_{ijkl}^E\, \varepsilon_{ij}\, \varepsilon_{kl}}_{\mathscr{U}_m} \underbrace{- e_{kij}\, E_k\, \varepsilon_{ij}}_{\mathscr{U}_{em}} \underbrace{- \frac{1}{2}\, \mathfrak{e}_{ij}^\varepsilon\, E_i E_j}_{\mathscr{U}_e} \tag{7}$$

In this expression, we can distinguish the pure mechanical energy density contribution $\mathscr{U}_m$, the electromechanical contribution $\mathscr{U}_{em}$ and the pure electrical contribution $\mathscr{U}_e$. It can be noticed that the mechanical contribution $\mathscr{U}_m$ in (7), can be expanded for pre-stress structures, as previously (4).

D. Dynamic Modelling for Pre-stress Piezoelectric Structure

The dynamics of the sensor device is available using energetic method and variational principle. In this paper, this is done using the *Hamilton*'s principle of least action and Lagrangian energetic function. The Lagrangian density of any electromechanical system is:

$$\mathscr{L}\left(u_i, \phi\right) = \mathscr{T}^* - \mathscr{U} + \mathscr{W} \tag{8}$$

where $\mathscr{T}^*$ is the kinetic co-energy density and $\mathscr{W}$ the work density done by external sources. For piezoelectric continuous media, the generalized displacements are mechanical displacements u_i and electric potentials ϕ. The *Hamilton*'s principle of least action states that:

$$\delta \mathscr{A} = \delta \int_{t_1}^{t_2} \int_V \mathscr{L}\, dV\, dt = 0 \tag{9}$$

for any virtual generalized displacements δu_i or $\delta\phi$. The solution of the related eigenvalue problem gives its natural frequencies and shapes (eigenvalues and eigenvectors).

In (8), the excitation energy density $\mathscr{W}$ from external sources are of different natures. They come from electrical stimulus (electric potential ϕ and $\bar{q}$ electric charge density) or mechanical forces density $\bar{f}_i^{ext}$, (Fig. 1):

$$\delta\mathscr{W} = \bar{f}_i^{ext}\,\delta u_i - \bar{q}\,\delta\phi \tag{10}$$

In (8), the kinetic co-energy density of a continuous media is defined as (with $\dot{u}_i = du_i/dt$):

$$\mathscr{T}^* = \rho\,\dot{u}_i\,\dot{u}_i/2 \tag{11}$$

This model takes into account the mechanics of the structure and the electromechanical coupling phenomena due to the piezoelectric elements. The internal energy density $\mathscr{U}$ in (8) for a system considering piezoelectric and pre-stress effects, can therefore be written as a result of (4-7):

$$\mathscr{U} = \mathring{\mathscr{U}}_k + \mathscr{U}_k + \mathscr{U}_n + \mathscr{U}_g + \mathscr{U}_{nl} + \mathscr{U}_{em} + \mathscr{U}_e \tag{12}$$

This energetic description allows us to describe the dynamic equations of the full sensor system. As stressed before, it is important to notice that the internal energy density (12), especially the geometric energy density $\mathscr{U}_g$, is a function of the to-be-measured force $\mathring{F}$. Therefore $\mathring{F}$ is linked to $\mathring{\sigma}$ which is linked to $\mathscr{U}_g$ and finally to the variational principle $\delta\mathscr{A} = 0$. The to-be-measured force $\mathring{F}$ is then directly embedded in the *Euler-Lagrange* equations and their modal shapes and frequencies. The solutions of this eigenvalue problem gives therefore a way to estimate the applied force $\mathring{F}$ and then to the use of the device as a multi-axis force sensor.

Nevertheless, *Euler-Lagrange* equations for continuous media have analytical solutions only in the case of very simple geometries, or 1-D approximations, such as beams. Because of this lack of analytical solutions for plates with arbitrary boundary conditions, the model of this pre-stress plate will be solved numerically using a Finite Elements Method in the next section.

III. FINITE ELEMENT MODELLING

A. Multilayer Plate Element Description

The plate is modelled using *Mindlin*'s theory, with the following assumptions:

- u_1 and u_2 displacements are linear functions of x_3 (linear displacements across the plate thickness, Fig. 3a).
- Stress σ_{33}, normal to the mid-plane, is negligible (null plane stress condition through the thickness: $\sigma_{33} = 0$) if normal components of external forces $\tilde{F}_3^{ext}$ are null.
- Surfaces, normal to the mid-plane before deformations remains straights after, but not necessary normal to this plane (θ_1 and θ_2 not necessary equal to $\frac{\partial u_3}{\partial x_1}$ and $\frac{\partial u_3}{\partial x_2}$, Fig. 3b and Fig. 3c) .

For numerical and Finite Elements computations, *Voigt*'s vector representation is commonly used instead of tensor one (Table II).

TABLE II
NOMENCLATURE FOR *Voigt*'S VECTOR QUANTITIES

Mechanical		Electrical	
$\{F\}$	Force	q	Electric Charge
$\{u\}$	Displacement	ϕ	Electric Potential
$\{\sigma\}$	Stress	$\{D\}$	Electric Displacement
$\{\varepsilon\}$	Strain	$\{E\}$	Electric Field

B. Finite Element Formulation

For a system with piezoelectric elements and considering pre-stressed initial conditions, the *Hamilton*'s principle (9) (with Lagrangian (8) including kinetic (11), external (10) and potential (12) terms) can be written in *Voigt*'s vector form as [13], [20]:

$$\begin{aligned} 0 = -\int_{\mathring{V}} \Big[& \rho\,\{\delta u\}^T\{\ddot{u}\} - \{\delta\varepsilon^{(1)}\}^T\left[c^E\right]\{\varepsilon^{(1)}\} \\ & - \{\delta\varepsilon^{(1)}\}^T\left[c^E\right]\{\varepsilon^{(2)}\} - \{\delta\varepsilon^{(2)}\}^T\left[c^E\right]\{\varepsilon^{(1)}\} \\ & - \{\delta\varepsilon^{(2)}\}^T\left[c^E\right]\{\varepsilon^{(2)}\} - \{\delta\varepsilon_g^{(2)}\}^T[\mathring{\sigma}]\{\varepsilon_g^{(2)}\} \\ & + \{\delta\varepsilon\}^T[e]^T\{E\} + \{\delta E\}^T[e]\{\varepsilon\} \\ & + \{\delta E\}^T[\ni]\{E\} + \{\delta u\}^T\left\{F_V^{ext}\right\}\Big]\,dV \\ & + \int_{\mathring{S}_m}\{\delta u\}^T\left\{F_S^{ext}\right\}dS - \int_{\mathring{S}_e}\delta\phi\,\bar{\sigma}\,dS \\ & + \{\delta u\}^T\left\{F_P^{ext}\right\} - \delta\phi\,Q \end{aligned} \tag{13}$$

$[\mathring{\sigma}]$ and $\{\delta\varepsilon_g^{(2)}\}$ are special matrix rearrangement terms described in [13] to take advantage of *Voigt*'s representation in the computation of $\mathscr{U}_g$. For clarity, superscript ˜ is omitted in this section (superscript ° is kept in the pre-stress matrix $[\mathring{\sigma}]$). Integrations are performed on pre-stressed volume $\mathring{V}$ and surface $\mathring{S}$.

Finite element method is based on a finite-dimensional reduction with interpolation functions defined on nodes of a mesh of the continuum. In the case of an electromechanical system, we consider that displacement $\{u\}$ and electric potential $\{\phi\}$ can be represented as a set of interpolation functions based on nodes values.

$$\{u\} = [N_u]\{u_i\} \tag{14a}$$

$$\{\phi\} = \left[N_\phi\right]\{\phi_i\} \tag{14b}$$

The strain $\{\varepsilon\}$ and electric $\{E\}$ fields can be therefore computed using numerical differential operators $[D]$ applied to the displacements and the electric potentials at the nodes:

$$\{E\} = \left[D_\phi\right]\left[N_\phi\right]\{\phi_i\} = \left[B_\phi\right]\{\phi_i\} \tag{15a}$$

$$\{\varepsilon_g^{(2)}\} = [D_g][N_u]\{u_i\} = [B_g]\{u_i\} \tag{15b}$$

$$\{\varepsilon^{(1)}\} = [D_u][N_u]\{u_i\} = [B_u]\{u_i\} \tag{15c}$$

$$\{\varepsilon^{(2)}\} = \sum_{\xi=1}^{5}\{u_i\}^T[B_g]^T\left[S^\xi\right][B_g]\{u_i\} = [B_{nl}(u_i)]\{u_i\} \tag{15d}$$

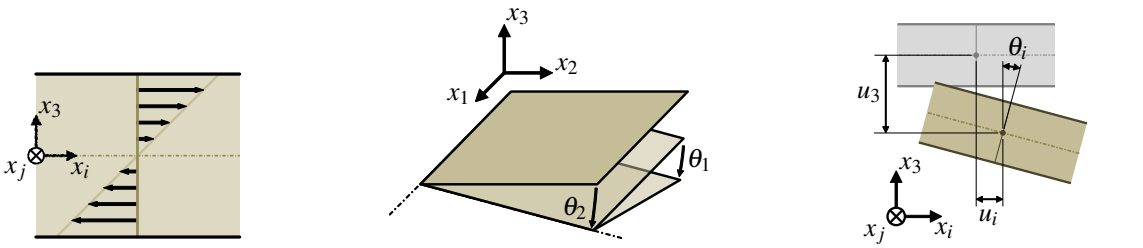

(a) linear displacement across the thickness (b) plate rotations (c) $x_3 \perp x_i$ plane displacements

Fig. 3. Representation of displacements of the plate according to the *Mindlin*'s kinetic assumptions: three translations u_1, u_2 and u_3, and two rotations θ_1 and θ_2. (with $i, j = \{1,2\}$ and $i \neq j$)

where, $[D_u]$ is the numerical differential operator such that $\{\varepsilon^{(1)}\} = [D_u]\{u\}$ according to (1). $[D_\phi] = -\nabla$ is the numerical gradient operator, and $[D_g]$ is a numerical differential operator described in [13]. The selection matrix $\left[S^\xi\right]$ rearranges each 2^{nd} order strain term of (1).

As seen before, (13) including (14) and (15) must be valid for any virtual admissible variation of displacement δu_i or electric field $\delta\phi_i$ [20]. This leads to the matrix equations for each element of the system:

$$\begin{aligned} [M]\{\ddot{u}_i\} + ([K_g] + [K_{uu}])\{u_i\} + \left[K_{u\phi}\right]\{\phi_i\} &= \left\{f_i^{ext}\right\} \\ \left[K_{\phi u}\right]\{u_i\} + \left[K_{\phi\phi}\right]\{\phi_i\} &= \{q_i\} \end{aligned} \tag{16}$$

where the mechanical stiffness $[K_{uu}]$ contains a non-constant term as follows :

$$[K_{uu}] = [K_l] + [K_{nl}(\{u_i\})]$$

Matrix of mass, geometry (pre-stress), mechanical stiffness, electromechanical coupling and electric capacitance are respectively defined as:

$$\begin{aligned} [M] &= \int_{\mathring{V}} \rho\,[N_u]^T[N_u]\,dV \\ [K_g] &= \int_{\mathring{V}} [B_g]^T[\mathring{\sigma}][B_g]\,dV \\ [K_l] &= \int_{\mathring{V}} [B_u]^T\left[c^E\right][B_u]\,dV \\ [K_{nl}] &= \int_{\mathring{V}} \Big([B_u]^T\left[c^E\right][B_{nl}] \\ &\quad + [B_{nl}]^T\left[c^E\right][B_u] \\ &\quad + [B_{nl}]^T\left[c^E\right][B_{nl}] \Big)\,dV \\ \left[K_{\phi u}\right]^T = \left[K_{u\phi}\right] &= \int_{\mathring{V}} [B_u]^T[e]^T\left[B_\phi\right]\,dV \\ \left[K_{\phi\phi}\right] &= -\int_{\mathring{V}} \left[B_\phi\right]^T[\mathfrak{s}^\varepsilon]\left[B_\phi\right]\,dV \end{aligned} \tag{17}$$

External forces and electric charges are defined as:

$$\begin{aligned} \left\{f_i^{ext}\right\} &= \int_{\mathring{V}} [N_u]^T\left\{F_V^{ext}\right\}\,dV \\ &\quad + \int_{\mathring{S}_f} [N_u]^T\left\{F_S^{ext}\right\}\,dS + [N_u]^T\left\{F_P^{ext}\right\} \\ \{q_i\} &= -\int_{\mathring{S}_q} \left[N_\phi\right]^T\bar{q}\,dS - \left[N_\phi\right]^T Q \end{aligned} \tag{18}$$

All the elements (16) can be assembled to obtain the matrix governing equations of the full system:

$$\begin{bmatrix} M & 0 \\ 0 & 0 \end{bmatrix}\begin{Bmatrix} \ddot{U} \\ \ddot{\Phi} \end{Bmatrix} + \begin{bmatrix} K_g + K_{UU} & K_{U\Phi} \\ K_{\Phi U} & K_{\Phi\Phi} \end{bmatrix}\begin{Bmatrix} U \\ \Phi \end{Bmatrix} = \begin{Bmatrix} F^{ext} \\ Q \end{Bmatrix} \tag{19}$$

$\{F^{ext}\}$ is the vector of external forces applied to the structure and $\{Q\}$ is the electric charges applied on the electrodes, the vector of unknowns is made by chaining the unknowns of each node as follows:

$$\{U\} = \sum_{i=1}^{n}\{u_i\} \quad \text{and} \quad \{\Phi\} = \sum_{i=1}^{n}\{\phi_i\}$$

As $[K_g]$ is a function of the measured force $\mathring{F}$, if a modal analysis of this system is performed, natural frequencies will be function of the to-be-measured force, according to our force sensor device principle.

Based on these analytical and numerical developments, and parts of codes from [21], this model has been implemented using the *MATLAB*® software. A case study is proposed in the following section to see the relevance of the method.

IV. CASE STUDY OF A COMPOSITE PLATE

Simulations are conducted to find the structure resonant frequencies for multiple configurations of pre-loads. Relationships between force and frequencies are then built with a two-steps procedure, as detailed in Algorithm 1. Computation of the relationship between resonant frequencies and input force is achieved sequentially:

- The static analysis can be used to check the maximal stress generated by the to-be-measured force. *Newton-Raphson* method has been used to solve the non-linearity due to $\left[K_{nl}(\mathring{U})\right]$.
- The modal analysis takes into account the strain field generated by $\mathring{F}$, and casts two kind of results that are used for different purposes: the *eigenvalues* (resonant frequencies) are used to set up the relationship between force and frequency. The *eigenvectors* (modal shape) are used to place optimally the sensors and actuators. This optimisation seeks to excite the structure with the minimum amount of energy and to get a high amplitude signal. In such a way, anti-nodes appear to be the best place to collocate the piezoelectric transducers.

Algorithm 1: Simulation steps to compute the relationship between resonant frequencies f_i and input force $\mathring{F}$ (steps are related with Fig. 2)

Input: Boundary conditions.
for $\mathring{F}$ **do**

1. *Static Analysis : Pre-stressing the structure*
Input: Force vector $\{\mathring{F}\}$
○ Calculation of the displacement field $\{\mathring{U}\}$ as solution of :

$$\{\mathring{U}\} = \left([K_l] + [K_{nl}(\mathring{U})]\right)^{-1}_{(V)} \{\mathring{F}\}$$

2. *Modal Analysis : Measuring the force via a frequency shift*
Input: Pre-stressed displacement field $\{\mathring{U}\}$
○ Calculation of the geometric matrix $[K_g(\mathring{\sigma})]$
- strain $\mathring{\varepsilon}$ calculation (15) from $\{\mathring{U}\}$
- stress $\mathring{\sigma}$ calculation via *Hooke*'s law
- Geometric stiffness $[K_g]$ (17)

○ Computation of resonant frequencies f_i :

$$([K_g] + [K_l] - \lambda [M])_{(\mathring{V})} \{U\} = 0$$

with, $\lambda = \omega^2$ and $\omega_i = 2\pi f_i$

end
Output: Mapping $\mathring{F} \rightarrow f_i$: resonant frequencies as a function of the input force

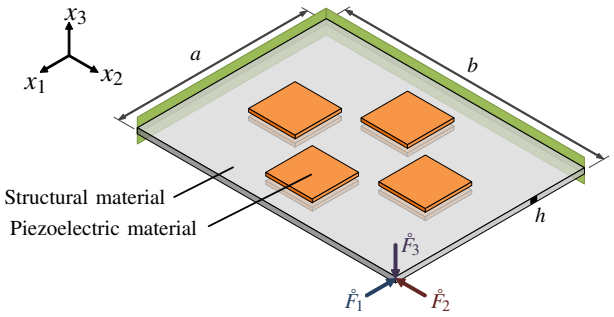

Fig. 4. Case study: composite rectangular plate with clamped conditions in two adjacent edges and a point of force $\mathring{F}$ applied at the free corner.

Due to the geometry of the structure, quadrangular shell elements (with 5 dofs) are used. The bonding between the passive structure and the piezoelectric elements is considered perfect (no glue layer is considered in this study). We assume that all piezoelectric patches are connected to electric ground ($\phi = 0$), and the stiffness due to the electrical contribution will not be considered in the following.

In Fig. 4, we present a simple case of a composite plate made of a passive material in the middle part, covered with piezoelectric patches on both faces. Two adjacent edges are clamped whereas the to-be-measured force, possibly multi-directional, is applied at the opposite corner. The dimensions and mechanical properties of the sensing device are reported in Table III. The simulation results of our *home-made* FE *MATLAB*® code are then compared with those of the commercial software *COMSOL*® *Multiphysics*.

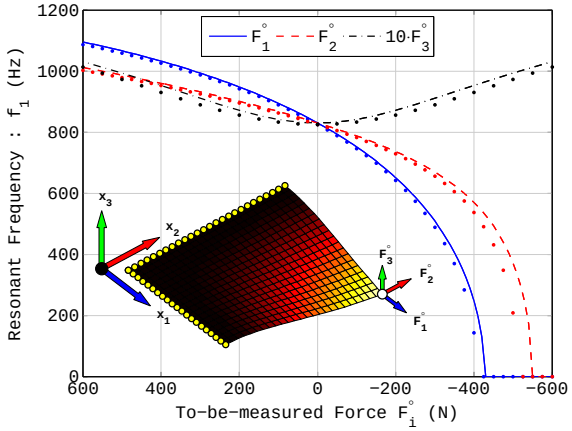

(a) First resonance around 834Hz, mode (1,1).

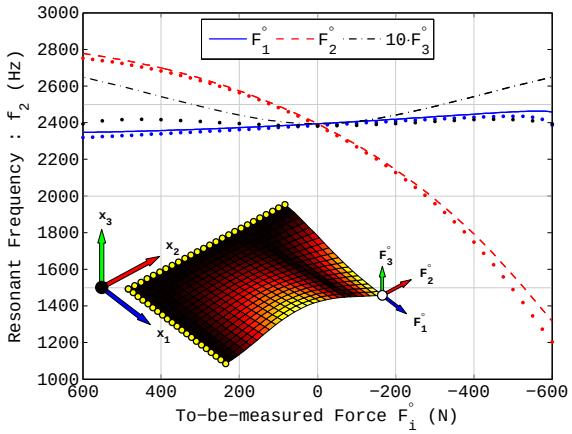

(b) Second resonance around 2487Hz, mode (1,2).

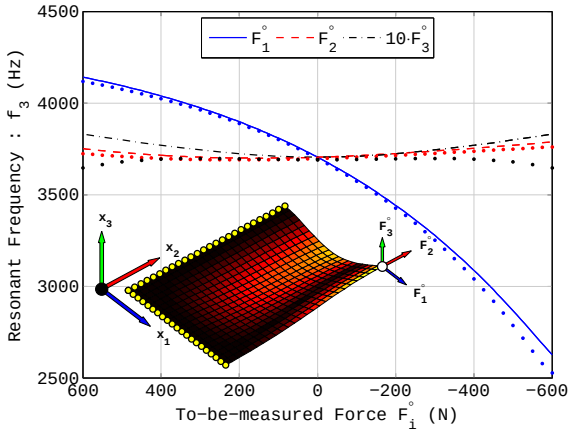

(c) Third resonance around 4232Hz, mode (2,1).

Fig. 5. Relationship between the three force components and the first three resonant frequencies for the case study structure (includes the force-free modal shape).

TABLE III

SIMULATION PARAMETERS

	Plate	Transducers
Dimensions		
length [m]	$4 \cdot 10^{-2}$	$1 \cdot 10^{-2}$
width [m]	$5.4 \cdot 10^{-2}$	$1 \cdot 10^{-2}$
thickness [m]	$5 \cdot 10^{-4}$	$2 \cdot 10^{-4}$
Material		
Elasticity modulus [GPa]	74	70
Poisson ratio [−]	0.33	0.3
Density [kg/m^3]	2790	7500

As can be seen in Fig. 5, the first three resonance frequencies are clearly sensitive to the to-be-measured forces $\mathring{F}$ and differently according to the three x_1, x_2 and x_3 axis. It is therefore possible to use this device as a multi-directional force sensor.

Fig. 5(a) shows that the first resonant mode can be used to sense the external force along the three directions ($\mathring{F}_1$, $\mathring{F}_2$, $\mathring{F}_3$) whereas the second (respectively the third) is not adapted to track the external force along the x_2 direction (respectively x_1 direction): the resonant frequency shift is less sensitive to $\mathring{F}_1$ (respectively $\mathring{F}_2$) applied force.

Because of the symmetry of the structure in the x_3 direction, the orientation (+ or -) of the to-be-measured force $\mathring{F}_3$ along the x_3 axis can not be distinguished by the shift frequency (only its amplitude is available). Indeed, the force in this direction will be seen as a tensile force irrespective of its orientation and this will increase the resonant frequency. But, this could certainly be overcome with an intelligent extraction algorithm or a fusion of additional rough static informations. Compared with *COMSOL® Multiphysics* simulations, our *home-made* finite elements code gives similar results, especially for the x_1 and x_2 force axis. It can therefore be used with confidence for the design and calibration of such kind of force sensor devices.

V. CONCLUSIONS

This paper presents the concept of a new multi-axis force sensor. This one is based on pre-stress resonant composite plates and is an interesting and viable alternative to the commonly used strain gauge sensor. The case study proves that such kind of sensors are able to measure the three components of an externally applied force.

Moreover, as electric charge are constantly generated in the dynamic steady state working mode of this device, inexpensive electronic instrumentation can be used, on the contrary of strain gauge or static piezoelectric force sensor devices.

The next steps of this work will be the experimental validation of these results using a prototype currently under construction.

REFERENCES

[1] X. Lamy, F. Colledani, F. Geffard, Y. Measson, and G. Morel, "Human force amplification with industrial robot : Study of dynamic limitations," in *2010 IEEE/RSJ International Conference on Intelligent Robots and Systems (IROS)*, pp. 2487–2494, 2010.

[2] K. Kosuge, Y. Fujisawa, and T. Fukuda, "Control of robot directly maneuvered by operator," in *Proceedings of the 1993 IEEE/RSJ International Conference on Intelligent Robots and Systems '93, IROS '93*, vol. 1, pp. 49–54 vol.1, 1993.

[3] D. M. Stefanescu, *Handbook of Force Transducers: Principles and Components*. Springer, Jan. 2011.

[4] D. Chapuis, R. Gassert, L. Sache, E. Burdet, and H. Bleuler, "Design of a simple mri/fmri compatible force/torque sensor," in *Intelligent Robots and Systems, 2004. (IROS 2004). Proceedings. 2004 IEEE/RSJ International Conference on*, vol. 3, pp. 2593–2599 vol.3, 2004.

[5] F. Sinden and R. Boie, "A planar capacitive force sensor with six degrees of freedom," in *Robotics and Automation. Proceedings. 1986 IEEE International Conference on*, vol. 3, pp. 1806–1814, 1986.

[6] D. Wang, Y. Zhang, C. Yao, J. Wu, H. Jiao, and M. Liu, "Toward force-based signature verification: A pen-type sensor and preliminary validation," *Instrumentation and Measurement, IEEE Transactions on*, vol. 59, no. 4, pp. 752–762, 2010.

[7] Y. Zhao, T. Zhao, R. Wen, and H. Wang, "Performance analysis and optimization of sizable 6-axis force sensor based on stewart platform," in *Mechatronics and Automation, 2007. ICMA 2007. International Conference on*, pp. 2189–2193, 2007.

[8] W. Fleming, "Automotive torque measurement: A summary of seven different methods," *Vehicular Technology, IEEE Transactions on*, vol. 31, no. 3, pp. 117–124, 1982.

[9] F. Aghili, M. Buehler, and J. M. Hollerbach, "Design of a hollow hexaform torque sensor for robot joints," *Int. Journal of Robotic Research*, vol. 20, no. 12, pp. 967–976, 2001.

[10] M. Uchiyama, E. Bayo, and E. Palma-Villalon, "A systematic design procedure to minimize a performance index for robot force sensors," *Journal of Dynamic Systems, Measurement, and Control*, vol. 113, no. 3, pp. 388–394, 1991.

[11] A. Cheshmehdoost and B. Jones, "Design and performance characteristics of an integrated high-capacity DETF-based force sensor," *Sensors and Actuators A: Physical*, vol. 52, pp. 99–102, Mar. 1996.

[12] K. Fukuzawa, T. Ando, M. Shibamoto, Y. Mitsuya, and H. Zhang, "Monolithically fabricated double-ended tuning-fork-based force sensor," *Journal of Applied Physics*, vol. 99, pp. 094901 –094901–5, May 2006.

[13] R. D. Cook, D. S. Malkus, M. E. Plesha, and R. J. Witt, *Concepts and Applications of Finite Element Analysis*. John Wiley & Sons Inc, 4th international student edition ed., Oct. 2001.

[14] D. Wang, L. Fang, M. Xu, and J. Yu, "Flexible building blocks: Modularized design concept of a six-axis force/torque sensor," in *Proceedings of the 2011 IEEE International Conference on Mechatronics and Automation*, pp. 1109–1114, 2011.

[15] M. Geradin and D. Rixen, *Mechanical vibrations: theory and application to structural dynamics*. Chichester; New York: John Wiley, 1997.

[16] L. D. Landau and E. M. Lifshitz, *Theory of elasticity*, vol. 7 of *Course of Theoretical Physics*. Oxford; New York: Pergamon Press, 2nd ed., 1970.

[17] H. Tiersten, "Hamilton's principle for linear piezoelectric media," *Proceedings of the IEEE*, vol. 55, no. 8, pp. 1523–1524, 1967.

[18] R. C. Smith, *Smart material systems: model development*. Philadelphia: Society for Industrial and Applied Mathematics, 2005.

[19] L. D. Landau, E. M. Lifshitz, and L. Pitaevskii, *Electrodynamics of Continuous Media*, vol. 8. Oxford; New York: Pergamon Press, 2 ed., 1979.

[20] V. Piefort and A. Preumont, "Finite element modeling of piezoelectric structures," in *Samtech User's Conference*, (Paris, France), Jan. 2001.

[21] A. J. M. Ferreira, *MATLAB codes for finite element analysis solids and structures*. Dordrecht; London: Springer, 2008.